Mechanical properties of ternary lipid membranes near a liquid–liquid phase separation boundary

FAST TRACK COMMUNICATION

Mechanical properties of ternary lipid membranes near a liquid–liquid phase separation boundary

Young Zoon Yoon[1,2]**, John P Hale**[3]**, Peter G Petrov**[3] **and Pietro Cicuta**[2]

[1] Department of Physics, Sungkyunkwan University, Suwon 440-746, Korea
[2] Cavendish Laboratory and Nanoscience Centre, University of Cambridge, Cambridge CB3 0HE, UK
[3] School of Physics, University of Exeter, Exeter EX4 4QL, UK

E-mail: pc245@cam.ac.uk

Abstract
We study the mechanical properties of ternary lipid bilayers assembled in giant vesicles, formed from a saturated and an unsaturated phosphocholine (in equal proportions) and cholesterol. As a function of temperature, these systems can undergo in-plane phase separation. Using image analysis we identify the vesicle contour, and quantify the vesicle shape and the amplitude of membrane thermal fluctuations. The two lipid compositions chosen show different thermotropic behaviours. At 60 mol% cholesterol the membrane is in a uniform liquid state over the entire temperature range investigated (10–50 °C), but vesicles containing 30 mol% cholesterol undergo phase separation into two immiscible liquid phases at around 28 °C. Upon cooling below this transition temperature we observe a marked increase in the measured bending elastic modulus. Phase separation proceeds over a long time (tens of minutes), and we measure the properties of vesicles both during the domain coarsening phase and in the fully phase separated condition. Fluorescence microscopy allows us to identify the coexisting phases. We can therefore measure directly the bending moduli of each of the phases as a function of temperature, showing a strong variation which is attributed to the changing phospholipid and cholesterol composition.

S Supplementary data are available from stacks.iop.org/JPhysCM/22/062101/mmedia

(Some figures in this article are in colour only in the electronic version)

1. Introduction

The plasma membrane of mammalian cells contains more than a hundred different lipid species [1, 2] and one of the major challenges to contemporary molecular biology and biophysics is to understand the functional significance of this molecular diversity [3–6]. This is of primary importance since it is now recognized that many essential cell functions such as transport, energy transduction, signalling, cell recognition and motility [7, 8] partially or fully reside in the membrane.

The lipid bilayer, originally envisaged as merely a matrix for embedding the membrane proteins, is now thought, on the basis of supporting experimental evidence, to contribute to membrane function via its effect on protein conformation, stability, assembly and distribution [9]. The question of the lateral organization of the lipid molecules in the membrane and its effect on protein function is therefore of much interest and significant research in the field is dedicated to studying lipid rafts, believed to be key elements in a number of membrane-related processes (there are some excellent reviews on the

subject, e.g. [2, 10]). This research has also highlighted the necessity of better understanding the coupling between membrane molecular composition and its phase state and lateral organization, on molecular to mesoscopic length scales, as related to its biological functions. For example, it has been shown both theoretically and experimentally that the lipid bilayer mechanical properties can control and direct membrane protein function [11–14].

Model systems, such as Langmuir monolayers spread on aqueous surfaces, lipid vesicles and supported bilayers, provide essential similarity to the plasma membrane bilayer yet are sufficiently reduced in complexity to allow processes such as lateral phase separation in the plane of the membrane, equilibrium and transient domain structure and their relation to membrane viscoelastic properties to be understood in terms of generic and specific physical interactions. This is the approach taken in the present work. We study model membranes containing a ternary lipid mixture of a saturated phosphocholine (DPPC), an unsaturated phosphocholine (DOPC) and cholesterol, which have been shown to undergo liquid–liquid phase separation as a function of temperature [15–18], and monitor changes in the elastic bending properties of the membrane in response to lateral phase separation. This transition is different from the 'main transition' between gel and liquid phases, where the mechanics also changes drastically [19]. The system of choice models two important features of the much more complex native cell membrane. First of all, in plasma membrane cholesterol is believed to be responsible for the formation of the so-called 'liquid–ordered' (L_o) phase through its interaction with sphingolipids and glycerophospholipids [20, 21]; coexistence between liquid–ordered (L_o) and a liquid–disordered (L_α) phases in ternary mixtures including cholesterol (with compositions similar to those used here) has been demonstrated in model bilayer systems [15–17, 22, 23]. Secondly, and very interestingly, it has been suggested [10, 15–17, 24] that membrane lipid composition may be close to liquid–liquid (L_o–L_α) miscibility critical point. If this is the case, then slight changes in temperature, lipid or protein composition or solute concentrations may trigger domain formation as required for specific cell functions, and furthermore even in the mixed state there will be large transient concentration fluctuations. However, this process is also likely to entail a coordinated change in the mechanical properties of the membrane as a part of the regulatory mechanism. It is therefore important to clarify how lateral phase separation and domain formation relate to membrane mechanical properties. We chose to study this in a model bilayer system (giant vesicles) by forcing the system from a single phase to L_o–L_α phase coexistence whilst monitoring the relevant membrane elastic properties. The behaviour of this system is also compared and contrasted with that of a similar system where no phase separation takes place. Membrane thermal fluctuations have been measured as a non-invasive probe of membrane mechanics. This is a well known approach, and a brief review is given in the supplementary materials (SM1 available at stacks.iop.org/JPhysCM/22/062101/mmedia).

We investigate membrane mechanical properties in two different situations. Immediately after reducing the temperature below the liquid–liquid phase separation temperature, one observes spinodal decomposition resulting in a number of micrometre-sized domains of a minority liquid phase embedded in a matrix of the continuous liquid phase. This state can be observed over a period of many minutes, which allowed us to record the thermal fluctuation behaviour of the composite membrane and therefore characterize the overall change in the membrane mechanical and thermomechanical properties. We interpret the membrane fluctuations in terms of an *effective* bending rigidity since, strictly speaking, this property can only be defined unambiguously for a single phase. Due to the qualitative nature of the effective property, this part of the study is presented in the supplementary materials (SM2 available at stacks.iop.org/JPhysCM/22/062101/mmedia). We focus here on the system which is established on a longer timescale (tens of minutes). The individual domains of the minority phase have diffused and coalesced until the membrane phase became composed of just two domains of comparable size. Such vesicles are used to characterize the membrane mechanical properties for each existing phase separately, and as a function of temperature.

2. Experimental methods

2.1. Giant vesicles

Phospholipids, 1,2-dipalmitoyl-*sn*-glycero-3-phosphocholine (DPPC) and 1,2-dioleoyl-*sn*-glycero-3-phosphocholine (DOPC) (Avanti Polar Lipids, USA) and di-hydro-cholesterol (Sigma, USA) were stored at −20 °C and used without further purification for preparation of giant vesicles. Stock solutions of all lipids were diluted to 5 mg ml^{-1} in a mixed solvent of 2:1 (vol/vol) chloroform:methanol. A nominal amount (~1 mol%) of NBD-tagged lipid (NBD C12-HPC, cat. No. N3787, Invitrogen, UK) was added for fluorescent imaging. We used two different ternary mixtures for the preparation of giant vesicles, which show different thermotropic behaviour. For a mixture of 1:1 DOPC:DPPC + 30%(mol) cholesterol, the lipid bilayers exhibit a clear phase separation into a continuous condensed phase and discrete islands of a more disordered phase below ~28 °C, whereas at 1:1 DOPC:DPPC + 60%(mol) cholesterol only a single uniform liquid crystalline phase is sustained over the entire temperature range investigated (10–50 °C). This behaviour is illustrated by the schematic phase diagram in figure 1, where the fluorescent images clearly demonstrate the phase separation in a vesicle formed by 1:1 DOPC:DPPC + 30%(mol) cholesterol. Quasispherical giant vesicles (30–50 μm in diameter) were prepared by the electroformation method [15, 25]. A chamber was constructed with a pair of conducting indium tin oxide (ITO)-coated glass microscope slides of resistance <20 Ω (VisionTek Systems, UK). Vesicles were formed in 197 mM sucrose solution after incubating the system for more than 2 h at 45 °C whilst applying an oscillating electric field (1.0 V, 10 Hz, produced using a function generator). The vesicles were re-suspended in 200 mM glucose (producing the same osmotic
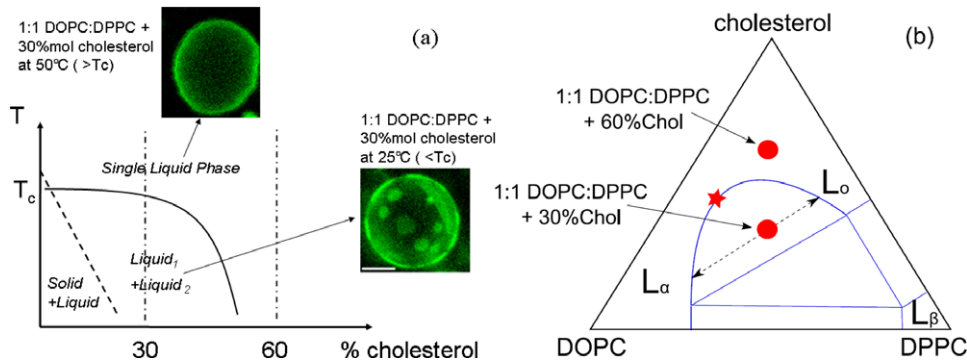
Figure 1. Schematic phase diagrams of the ternary systems investigated in terms of (a) cholesterol concentration, and (b) ternary composition at a fixed temperature below T_c. Both diagrams are schematic, based on data in [15–17]. (a) illustrates the temperature quench to a temperature below the phase transition boundary; the confocal fluorescence microscopy images show the same vesicle in its homogeneous single-phase state (at $T > T_c$) and immediately after the onset of phase separation (at $T < T_c$) when newly formed domains are visible as bright spots. The two compositions studied in this work are marked in (b) with red dots and their respective thermal trajectories are represented with vertical lines in (a). The star indicates the critical point.

pressure) in an attempt to obtain a refraction index mismatch; however, in the course of the experiments we observed loss of contract between the inside and outside of the vesicles due to (slow) content exchange.

2.2. Microscopy

Vesicles were observed using a Zeiss LSM510 confocal microscope, equipped with a $50\times$ phase objective. The fluorescence mode was initially used to determine phase separation boundaries, and then image series were recorded in phase contrast on a CCD camera at 25 frames per seconds to be used in the thermal fluctuation analysis. Occasionally we used a Leica TCS SP5 confocal microscope with $100\times$ and $63\times$ oil immersion objectives and a 488 nm laser in fast resonant scanning mode (8 kHz line scanning frequency). Images from this microscope were recorded at 512 pixels $\times$ 512 pixels and a frame rate of 15 frames s^{-1}. At this magnification the pixel size was of the order of 50 nm. Due to the fast line scanning, the time delay between acquiring neighbouring pixels was at most 1.25×10^{-4} s, which avoids many of the complications due to finite exposure times [26]. Using the Leica microscope, the confocal epi-fluorescence image and the transmitted phase contrast intensity were recorded simultaneously.

The temperature was varied between 10 and $50\,^\circ$C with a temperature control system (Linkam, UK), following different thermal paths as described below. Samples were allowed to reach thermal equilibrium for a few minutes at each new temperature before the acquisition of the video sequences. Using the oil immersion objective, it was important to monitor the temperature within the sample. This was done by calibrating the set temperature against the actual sample temperature, measured with a small thermal probe in contact with the sample cell.

Up to 2000 vesicle contours were captured at each temperature, and either 100 or 200 frames at a time were analysed to extract independent values for the bending modulus, as described below. The fluctuating membrane contour was detected by an algorithm developed in-house and coded in Matlab.

2.3. Fluctuation analysis

The fluctuation spectrum for planar membranes can be calculated in the continuous limit, taking into account the membrane bending modulus and tension [27]. The classical calculation is reproduced in supplementary materials section SM1 (available at stacks.iop.org/JPhysCM/22/062101/mmedia), to clarify the notation used. In optical microscopy experiments, only the fluctuations of the vesicle in the plane of its equator are observable. These can be calculated from equation S3 by means of a transform from Fourier space into real space for one of the spatial coordinates (e.g. y), as calculated in [26], giving

$$\langle h(q_x, y=0)^2 \rangle = \frac{1}{L} \frac{k_B T}{2\sigma} \left[\frac{1}{q_x} - \frac{1}{\sqrt{\frac{\sigma}{\kappa} + q_x^2}} \right]. \quad (1)$$

It can be seen from equation (1) that for typical values of the bending modulus (20–50$k_B T$) and q_x range (10^5–10^6 m^{-1}), the membrane tension σ affects the spectrum only if it is greater than $\sim 10^{-8}$ N m^{-1}. For bending-dominated fluctuations, $\sigma/(q_x^2\kappa) \to 0$, the spectrum reduces to

$$\langle h(q_x, y=0)^2 \rangle = \frac{1}{4L} \frac{k_B T}{\kappa q_x^3}. \quad (2)$$

We find that equation (2) describes well our data for quasispherical vesicles in the region 2×10^5 m^{-1} $< q < 1 \times 10^6$ m^{-1}, i.e. between modes 6 and 20 (see figure SM1 available at stacks.iop.org/JPhysCM/22/062101/mmedia). Lower modes (up to mode 5) are affected by membrane tension as well as the membrane overall spherical geometry, and high modes (above 20) are impossible to detect reliably due to the limited optical resolution, their fast relaxation rate and the camera noise. A detailed discussion on the applicability of equation (2) to the analysis of quasispherical vesicle fluctuations and its limitations can be found in [26]. We used our approach recently to study red blood cell membrane fluctuations [28].

Membrane contours are extracted by detecting the minimum of intensity in the sigmoid shape of the grey level
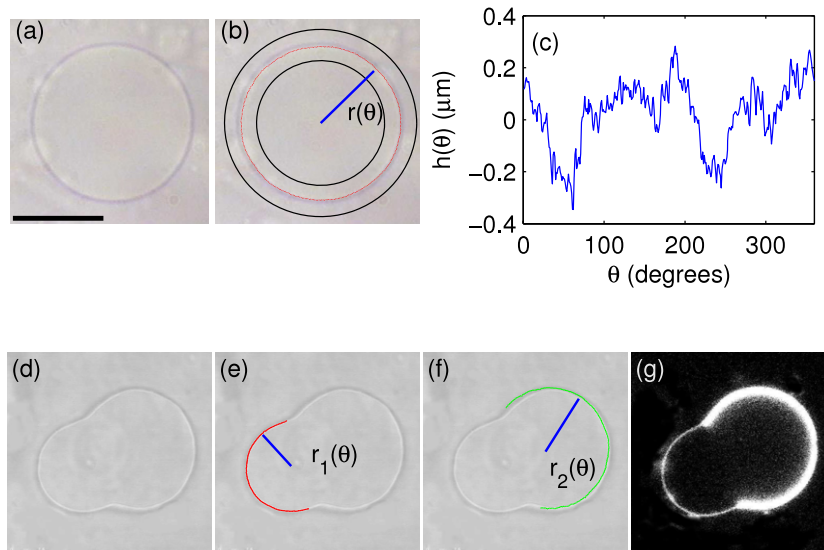
Figure 2. (a) Snapshot of a giant quasispherical vesicle in phase contrast microscopy; (b) procedure for contour detection; the inner and outer search bounds are given by solid lines, and the automatically detected contour points are shown as dots; (c) fluctuation amplitude $h(\theta)$; the distance between the value in a particular frame and the mean position over time as a function of the angle θ; (d) snapshot of a fully phase separated giant vesicle, consisting of two quasispherical segments; (e) contour detection of the L_o phase; (f) contour detection of the L_α phase; (g) fluorescence image of the phase separated vesicle. The brighter part of the membrane is the L_α phase. The scale bar is 20 μm.
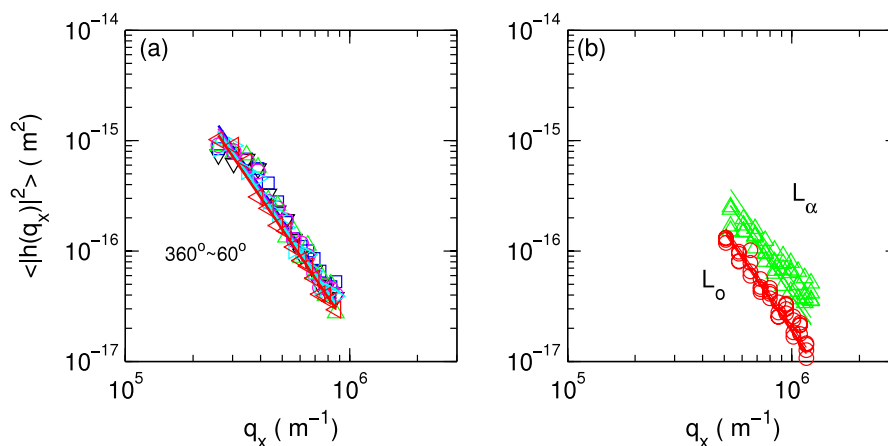

Figure 3. An arc of contour is sufficient for analysing fluctuation amplitudes, as shown in panel (a), where data from the same spherical vesicle as in figure SM1(a) (available at stacks.iop.org/JPhysCM/22/062101/mmedia) at 308 K are reported after selection of a decreasing arc of angles from 360° to 60° in 60° steps. Fluctuation amplitudes of coexisting phases are shown in (b), for a budded vesicle of composition 1:1 DOPC:DPPC + 30 mol% cholesterol, at 283 K. Markers correspond to different phases, and various data sets are shown for each phase, obtained from independent sets of images. The solid lines correspond to the fit of the data using equation (3).

profile across the membrane. As described in [26] this can be done by fitting a linear function to the profile, leading to sub-pixel resolution. We used polar coordinates with the origin in the contour centre, so that the contour shape is described by $r(\theta)$; see figure 2.

We emphasize that equation (2), despite being strictly valid for a planar fluctuating membrane, can still be used in the case of quasispherical vesicles apart from the first five modes, as discussed in detail in [26, 29], without compromising the accuracy of measurement. This is due to the fact that to a good approximation only the first five modes of the discrete series (not shown on figure 3) are affected by the curvature and closed topology of the membrane. The comparison between the fluctuation spectra for a planar membrane and quasispherical vesicle shows no relevant difference for mode number larger than 5 [26, 29]. Data are fitted up to the wavevector where noise in the spectra due to limited resolution of the contour position becomes appreciable (around $q_x \approx 10^6$ m^{-1} for data obtained using the Zeiss microscope, and $q_x \approx 2 \times 10^6$ m^{-1} for data from the Leica microscope; see the methods section above). In summary, about 15 modes, starting from the sixth mode of the spectrum, are used to obtain the values of the membrane bending modulus.

We now consider the fluctuations of fully phase separated vesicles, formed of only two large coexisting domains of different composition (figures 2(d)–(g)). Our approach in
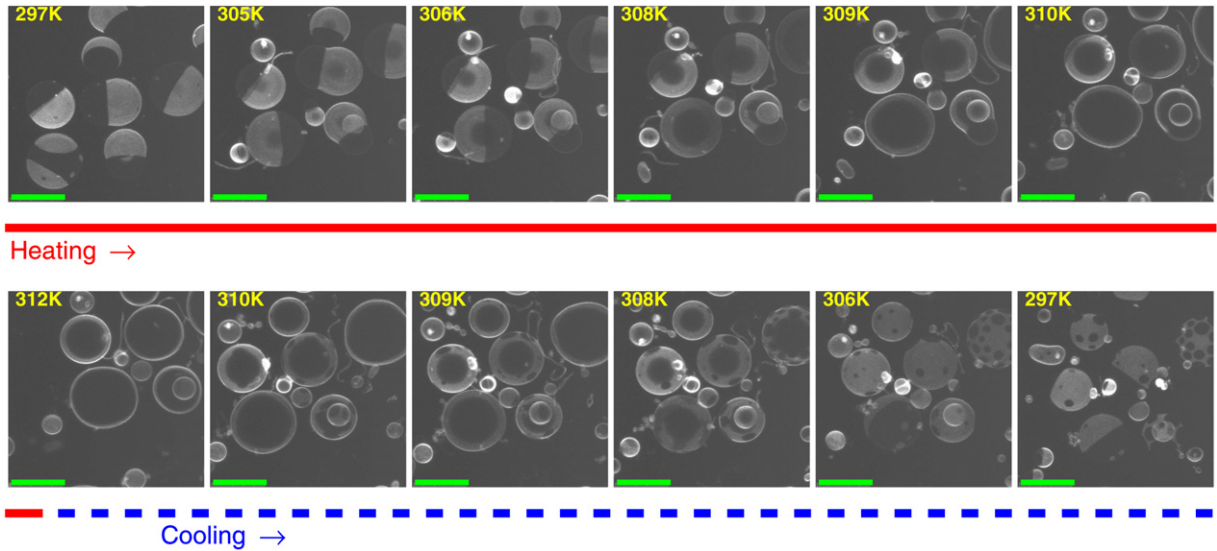
Figure 4. Wide field view of vesicles undergoing heating and cooling. It can be seen that T_c varies slightly between vesicles, but that for each vesicle the mixing and demixing T_c are the same. The scale bar is 20 μm.

analysing the membrane fluctuations in this case is similar to the one recently reported in [23]. The shape of these vesicles consists approximately of two spherical sections [23, 30]. Choosing vesicles oriented so that the equatorial section is made of two arcs, the fluctuations of the two sections can be analysed separately. This is similar to the quasispherical case, provided that the amplitude is normalized appropriately to account for the incomplete perimeter. If only an arc under angle θ is selected for analysis, then the mean square amplitude $\langle h'(q_x, y = 0)^2 \rangle$ is given by

$$\langle h'(q_x, y = 0)^2 \rangle = \left(\frac{2\pi}{\theta} \right) \frac{1}{4L} \frac{k_B T}{\kappa q_x'^3} \qquad (3)$$

where L is the complete circumference $2\pi \langle r \rangle$ as before, and the wavenumber range is reduced to $q_{x_k}' = \frac{1}{\langle r \rangle}(\frac{2\pi}{\theta}, \frac{2\pi}{\theta} + 1, \ldots, \frac{2\pi}{\theta} + \frac{N}{2})$, i.e. part of the low frequency range is lost compared to when the full equatorial contour is available (see SM1 available at stacks.iop.org/JPhysCM/22/062101/mmedia), but the high end and the resolution in q_x are maintained. The normalization in equation (3) can be understood by considering the selection of an arc as a 'zero padding' of the function h_n.

To validate this approach, we performed two checks. This first one was done on a single quasispherical vesicle. Starting with the full contour length, we measured the vesicle fluctuation spectra for a series of arches with decreasing length. Figure 3(c) demonstrates that the selected angle can be as low as 60° without greatly affecting the mean square amplitude of the fluctuations, i.e. the value of the bending modulus can reliably be recovered even from a selection of the circumference. This situation however is not fully equivalent to analysing vesicles consisting of two different domains, whose shape also depends on the Gaussian moduli of the two phases as well as the line tension γ. As shown in [23], each domain approaches a spherical shape away from the neck region (where the two phases are joined). The

size of the neck region where the line tension dominates the shape is given by κ_i/γ [31]. The results reported in [23] for liquid–liquid phase separated vesicles containing DOPC, brain sphingomyelin and cholesterol suggest a neck region size of less than a micrometre. Consequently, we adopted the following procedure. The selection of the angles corresponding to the parts of contour in each domain is done manually, and figures 2(e) and (f) show an example. The mean radius of curvature $\langle r \rangle$ in each phase is calculated as the mean radius of curvature over all frames. The centres of the two circumference sections are determined automatically by iterating the contour detection algorithm. The bending rigidity in each phase is calculated using equation (3). Again, to check the validity of this approach we performed a series of calculations for different arch lengths of each domain contour, and found a good agreement between the values of the bending modulus obtained; see figures 3(c) and (d). This proves that any deviations of the domain contour shape from spherical due to the effect of the line tension are confined close to the boundary and do not affect the measured fluctuation spectrum.

3. Results

3.1. The onset of phase separation

First we examined the phase behaviour of two systems (containing either 30% or 60% cholesterol) using confocal fluorescence microscopy. As can be seen from the snapshots in figure 4, at temperatures below $T_c \sim 35\,°C$ we observe a coexistence of isolated bright domains, embedded in a non-fluorescent continuous phase for the membrane consisting of 1:1 DOPC:DPPC + 30 mol% cholesterol. Since the fluorescent dye is expected to partition almost exclusively in the less condensed phase [15], we conclude that the system consists of a continuous L_o phase and discrete L_α domains. Increasing the temperature above T_c leads to a transition to

a uniform disordered liquid phase. In contrast, imaging the GUVs of composition 1:1 DOPC:DPPC + 60 mol% cholesterol confirms that there is one single liquid phase throughout the entire temperature range investigated. This behaviour is in agreement with the phase diagrams reported in the literature [15] (see also figure 1) and validates our composite vesicle preparation method. Lowering the temperature below T_c, the phase separation of the 30% sample proceeds via an initial stage of spinodal decomposition, and a later stage of domain diffusion and coalescence. This second stage is very slow, and it may take tens of minutes for all domains to coalesce and for the membrane to become just two coexisting domains of different phases [32].

3.2. Bending rigidity

Leaving the vesicle sample containing 30% cholesterol to equilibrate for a long time (tens of minutes to hours) leads in most cases to complete phase separation into two large domains of comparable areas, as can be seen in figure 4. In principle the coarsening process could be arrested, but only under special conditions [33] which we do not apply. Thermal cycling across the phase transition temperature results in reversible mixing–demixing for every vesicle in the sample. Close inspection of figure 4 reveals that the transition temperatures are slightly different for the different vesicles, although for each particular vesicle the transition temperature is highly reproducible. The absence of hysteresis is an interesting observation because it implies that the coupling of composition to curvature is insufficient to change the energy of the system enough for observing a measurable change in critical temperature as a function of vesicle shape. The variability between vesicles is again probably due to slight variations in the composition of different vesicles since, once formed, their membrane composition is arrested and no lipids can be exchanged between different vesicles.

By selecting vesicles consisting of two clearly formed spherical segments, it is possible to monitor their fluctuation amplitudes separately, which allows the measurement of the bending modulus of the L_o and L_α phases independently. The addition of cholesterol was shown to increase the phosphocholine bilayer bending rigidity [26, 34]. Previous studies of static shapes of liquid–liquid phase separated vesicles containing DOPC, egg sphingomyelin and cholesterol have established that the bending rigidity of the L_o phase is about five times higher than that of the L_α phase [35]. Absolute values of these two bending moduli for the system DOPC, brain sphingomyelin and cholesterol were recently reported in [23], confirming that the bending modulus of the L_o phase (8×10^{-19} J) is higher than that for the L_α phase (1.9×10^{-19} J). Our data provide a direct quantitative measure of the bending rigidities of these two phases in a system containing DOPC, DPPC and cholesterol, at various temperatures (and hence coexistence compositions on the phase diagram) and also extends the analysis to the vicinity of the critical point.

We find that as the temperature increases the bending rigidities of the two phases decrease and approach a similar value, as shown in figure 5. The fact that the values of the two
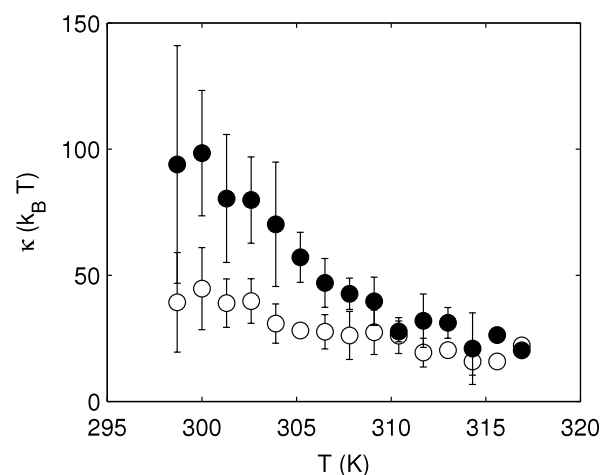

Figure 5. Temperature dependence of the bending rigidity κ for phase separated ternary membranes (GUVs) of composition 1:1 DOPC:DPPC + 30% cholesterol. Markers correspond to the L_o phase (●) and L_α phase (○). The value of κ at each temperature is an average from independent measurements for four different vesicles.

phases converge is expected, since the two phases approach the same compositions at the critical temperature. Interestingly, the bending rigidity of the L_o phase has a stronger temperature dependence than that of the L_α phase. This may be due to the 'trajectory' of the binodal line on the phase diagram, as temperature is changed: the phase diagram of figure 1 shows the binodal as a function of the composition and the L_α branch tends towards the critical point with increasing cholesterol, whereas the L_o branch reaches the critical point on increasing the unsaturated lipid fraction. The latter clearly has a stronger effect on the bending modulus. A similar trajectory can be expected as the temperature is varied [36].

The critical temperatures are slightly different for each vesicle and this fact can obscure the trend of the bending moduli as presented in figure 5. The analysis of the temperature trends for each vesicle separately, taking into account its particular transition temperature, shows that close to the mixing transition the bending modulus decreases linearly to a finite value, $\kappa(T) \simeq \kappa^{(0)}(1 - \tau T)$ (one example is shown in figure 6; for this vesicle $\kappa^{(0)} = (2.5 \pm 0.3) \times 10^{-18}$ J, $\tau = (3.12 \pm 0.02) \times 10^{-3}$ K^{-1} for the L_α phase, and $\kappa^{(0)} = (5.6 \pm 0.4) \times 10^{-18}$ J, $\tau = (3.15 \pm 0.01) \times 10^{-3}$ K^{-1} for the L_o phase).

3.3. The effect of temperature on vesicle morphology

The morphology of vesicles with intramembrane domains has been comprehensively described by Jülicher and Lipowsky [30]. The relevant parameters controlling vesicle shapes are the reduced line tension, $\lambda = \gamma R/\kappa_1$ and the relative domain size, $x = A_2/(A_1 + A_2)$, where the subscripts denote each domain. It is important to keep in mind that all these quantities are temperature dependent. Here γ is the line tension, R is the equivalent vesicle radius deduced from the total surface area ($4\pi R^2 = A_1 + A_2$), and A_i is the surface area of each domain. The reduced line tension λ measures the competition between the line energy at the boundary between
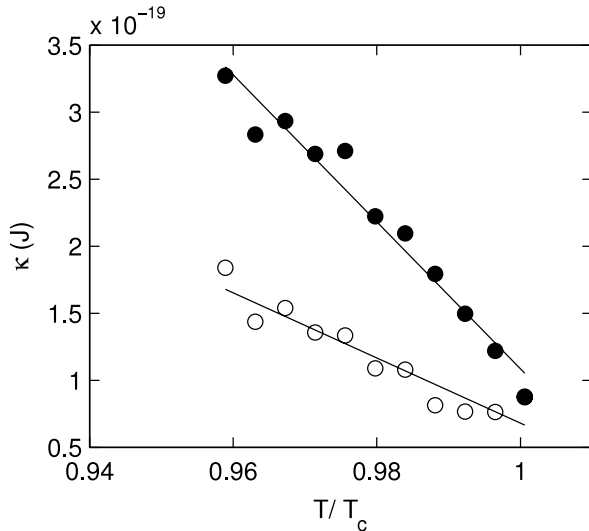
Figure 6. Temperature dependence of the bending moduli of the L_α (○) and L_o (●) phases for a single vesicle of composition 1:1 DOPC:DPPC + 30% cholesterol.

the two phases and the bending energy. Large values of the line tension favour the formation of a bud, provided also that the budding domain is large enough. At $\lambda = 0$ the shape of the vesicle is spherical. By increasing λ, one can form an incomplete bud (in Jülicher and Lipowsky's terminology) where the smaller domain forms a spherical cap on top of the bigger one. Upon reaching a critical value, $\lambda(x) = \lambda_D(x)$, the vesicle turns into a complete bud (two spherical segments connected with a neck of finite diameter). Finally, further increase of the reduced line tension leads to closing of the neck (at $\lambda(x) = \lambda_L(x)$); now the vesicle is composed of two spheres connected by an infinitesimally thin neck. In this way, vesicle shapes can be represented in a (λ, x) diagram. These authors derived analytical expressions for the critical parameters $\lambda_D(x)$ and $\lambda_L(x)$ for some special cases when no volume constraint is imposed on the system. The simplest case is obtained for domains of equal Gaussian bending moduli, equal bending rigidities, zero spontaneous curvatures, and no volume constraint, for which $\lambda_D(x) \simeq 2/\sqrt{x - x^2}$ and $\lambda_L(x) = (2/\sqrt{x}) + 2/\sqrt{1-x}$. For domains of equal size ($x = 0.5$), the transitions are expected to occur at $\lambda_D \simeq 4$ and $\lambda_L = 5.66$. A more realistic case that retains the differences in the bending moduli between the two phases are given by [30]

$$\lambda_D(x) \simeq \frac{\kappa_2}{\kappa_1} \frac{2}{\sqrt{x - x^2}} \left[x + \frac{\kappa_1}{\kappa_2}(1-x) \right] \qquad (4)$$

$$\lambda_L(x) = \frac{\kappa_2}{\kappa_1} \frac{2}{\sqrt{1-x}} + \frac{2}{\sqrt{x}}. \qquad (5)$$

Since most of the vesicles investigated here consist of domains of comparable sizes ($x \simeq 0.5$), the expected values of the critical parameters reduce to $\lambda_D = 2[1 + \kappa_2/\kappa_1]$ and $\lambda_L = 2\sqrt{2}[1 + \kappa_2/\kappa_1]$. The evaluation of these two parameters for the systems investigated here gave typical values of $\lambda_D \simeq 3.1$ and $\lambda_L = 4.4$.

Temperature can affect vesicle morphology through the intrinsic temperature dependences of the quantities involved in λ and x. To simplify the discussion, we will assume that the domains are of equal size and their coefficients of area thermal expansion are the same; this will ensure that $x = 0.5$ at all temperatures. We have measured the membrane thermal expansion coefficient, $\beta = (1/A_0)(dA/dT)$, from the linear parts of the temperature dependences of the vesicle area (see SM3 available at stacks.iop.org/JPhysCM/22/062101/mmedia). For vesicles containing 60% cholesterol the experimentally obtained values are $(7.6 \pm 0.9) \times 10^{-3}$ K^{-1}, $(4.7 \pm 1.0) \times 10^{-3}$ K^{-1}, and $(3.3 \pm 0.8) \times 10^{-3}$ K^{-1}, and a similar value, $(6.3 \pm 0.6)10^{-3}$ K^{-1}, is also obtained for the system containing 30% cholesterol. In this simplified situation, the only parameter controlling the vesicle shape is λ. Away from the critical temperature of mixing ($T \ll T_c$), the thermal trajectory of λ could be dominated by the thermal expansion of the area and the decrease of the bending rigidity: both of these factors will act to increase the reduced line tension λ. In this case, a vesicle starting from a low value of $\lambda < \lambda_D$ could evolve towards budding with increasing temperature. In many cases we observe experimentally such a trend (figure 7), but we warn the reader that this is *not* the first-order phase transition described by Jülicher and Lipowsky in [30]. This is explained further below. Increasing temperature towards $T \approx T_c$ will bring the vesicle closer to the mixing transition. The behaviour here will be dominated by the line tension γ which vanishes at T_c. We can always expect, therefore, a decrease in the value of λ to zero, which will carry a budded vesicle through a debudding transition. This is seen at temperatures close to T_c (figure 8).

Although the qualitative arguments given above provide a framework for discussing thermal shape trajectories of phase separated vesicles, comparison of the experimentally determined values of λ (see figure 9) with the critical values of λ_D and λ_L from equations (4) and (5) are in very obvious quantitative disagreement. In most cases, the experimental values of λ are very large, suggesting that the vesicles should consist of two spherical parts, fully budded, even in cases where we only observe a limited bud. This discrepancy is most probably due to the assumptions used in the theory to derive the approximate expressions for the critical values of λ, notably not imposing the constant volume constraint which will act to oppose the budding transition [30].

A semi-quantitative comparison between experiment and theory is justified in the immediate vicinity of T_c where λ can be estimated using linear temperature dependences of the parameters involved. To calculate λ, we assume linear area expansion and a linear decrease in the bending modulus (which we justified in figure 6). The temperature dependence of the line tension for this particular system (DOPC, DPPC, cholesterol) is not known. To estimate it, we will use a recently obtained dependence for the closely related DPPC, diPhyPC and cholesterol system, which also forms domains of liquid–ordered and liquid–disordered phases [22]. For this system it was found that $\gamma(T) = \gamma_0(1 - T/T_c)$ with $\gamma_0 \approx 25$ pN. The linear term in the expansion of $\lambda(T)$ for $T \to T_c$ is then given
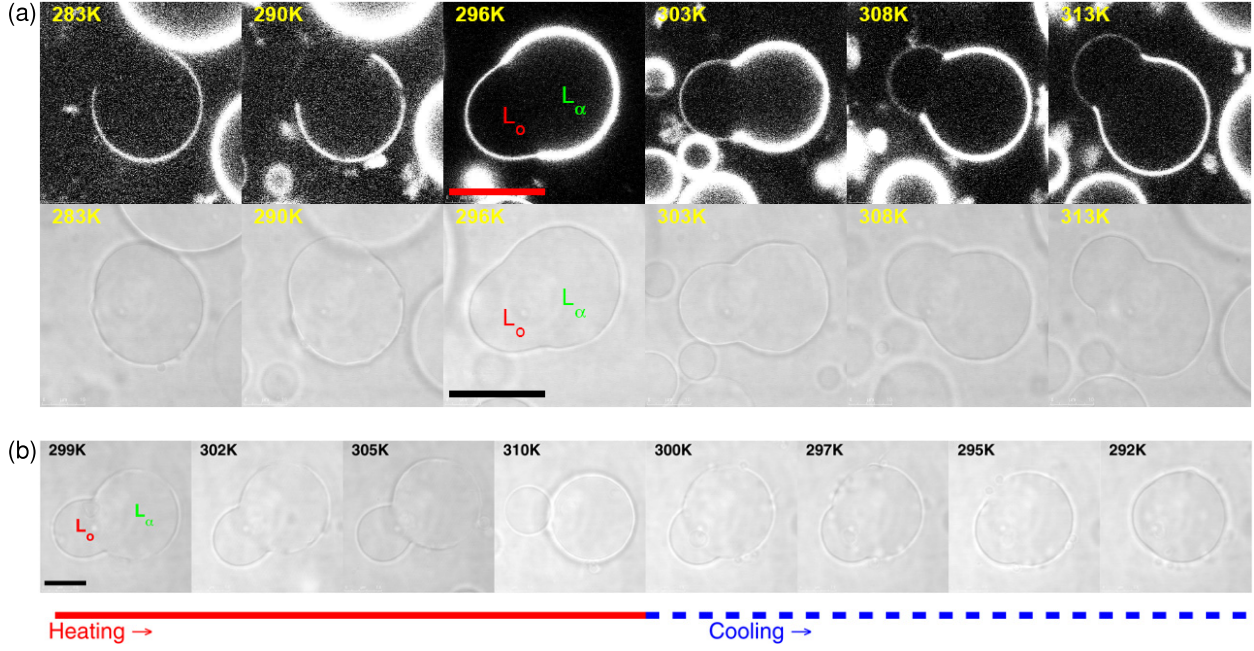
Figure 7. Two examples of budding process caused by increasing temperature. (a) formation of a bud with a finite neck diameter on heating; (b) reversible formation of a complete bud with an infinitesimally small neck upon heating and cooling.
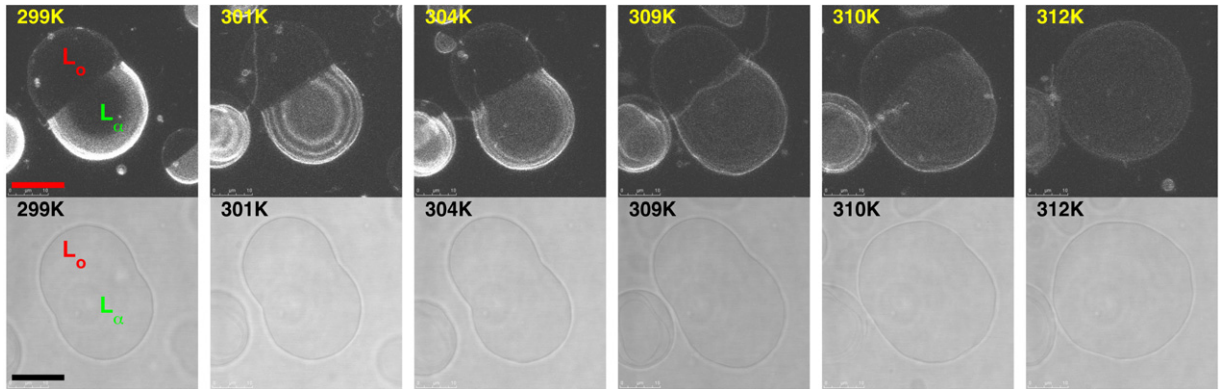

Figure 8. Example of a de-budding process upon heating very close to the critical temperature.

by

$$\lambda(T) \simeq \frac{\gamma_0 R_0}{\kappa_1^{(0)}} \frac{\sqrt{1+\tilde{\beta}}}{1-\tilde{\tau}} \left(1 - \frac{T}{T_c}\right) \quad (6)$$

where γ_0, $\kappa_1^{(0)}$ and R_0 can be evaluated from the linear temperature dependences of the line tension, bending modulus and area, respectively, $\tilde{\beta} = \beta T_c$ is the dimensionless area expansion coefficient, and $\tilde{\tau} = \tau T_c$ gives the rate of change of the bending modulus with temperature ($\tau = -\frac{1}{\kappa^{(0)}} \frac{d\kappa}{dT}$).

The experimental values of λ at each temperature are obtained using the measured values of the bending modulus and the equivalent radius. We used the above linear relationship for $\gamma(T)$ assuming that it is adequate as an estimate of this parameter in our case. The biggest uncertainty in the experimental estimation of λ is the error of measurement of the area of the two domains. This is due to the fact

that, for a faithful evaluation of the area, the vesicle must expose its exact meridional profile, which is not always the case due to the rotational diffusion of the whole vesicle (the area of quasispherical vesicles is much easier to measure due to the rotational invariance of their shape). In many cases measurement of the area of budded vesicles as a function of temperature produced non-monotonic trends due to such measurement artefacts. Due to these limitations, the comparison between the experimentally obtained thermal trajectories of λ and those estimated using equation (6), given in figure 9, should be considered only as semi-quantitative. Figure 9 shows the measured temperature dependences of λ for two different vesicles. In one of the cases both an increasing and a decreasing temperature dependence are observed. The solid lines represent the behaviour of λ according to equation (6), which should be valid for temperatures close to T_c. It could be seen that despite the numerous assumptions
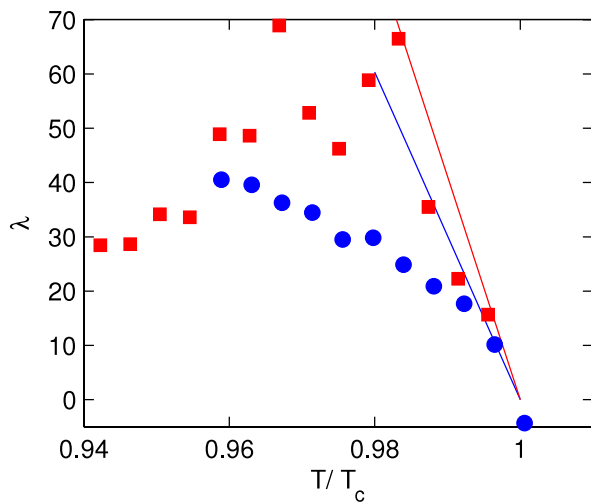
Figure 9. Temperature dependence of the reduced line tension λ for two vesicles. The solid lines show the trend of equation (6) with the following parameters: $\gamma_0 = 25$ pN, $\beta = 5 \times 10^{-3}$ K^{-1} are common values for the two vesicles; for the vesicle denoted with ■, $\kappa_1^{(0)} = 7.4 \times 10^{-18}$ J, $T_c = 317$ K, $\tau = 3.13 \times 10^{-3}$ K^{-1} and $R_0 = 7.1$ μm; for the vesicle denoted with ●, $\kappa_1^{(0)} = 5.6 \times 10^{-18}$ J, $T_c = 311.5$ K, $\tau = 3.15 \times 10^{-3}$ K^{-1} and $R_0 = 8.2$ μm.

made for estimating λ both theoretically and experimentally, there is a good agreement for temperatures approaching the critical one.

4. Discussion

We first compare the values of the effective bending moduli for the composite membranes to the bending rigidity of DOPC and DPPC single-component bilayers. Whereas the bending modulus for pure DOPC bilayers in the L_α state is within the expected range for a liquid membrane ($(4-15)$ $k_B T$ as reported in [37]), the saturated lipid DPPC has a more complex behaviour at temperatures similar to these investigated here due to the higher gel to liquid crystalline phase transition point. Lee *et al* [38] report an order of magnitude stiffening of DPPC membranes when they are forced through the liquid crystalline to gel transition. The measured bending modulus above 43 °C was ∼29$k_B T$ and sharply increased above $200k_B T$ at temperatures lower than 34 °C. The latter is comparable to the values of the effective bending modulus for the phase separated membrane (also rising above $150k_B T$) observed by us at low temperatures for the 1:1 DOPC:DPPC + 30 mol% cholesterol system, which is not surprising taking into account the high concentration of DPPC in the continuous phase of the composite membrane. The precise role of cholesterol is still not completely resolved [39]. Nevertheless it is clear that cholesterol does modulate the properties of the condensed lipid phases, as we observed in a comparative experiment: despite the high bending rigidity, we are still able to detect membrane thermal fluctuations in the composite system, but vesicles prepared from 1:1 DOPC:DPPC with no cholesterol exhibit no detectable undulations. For the latter system, it is known that the phase separation in the binary mixture is into a coexisting gel (L_β) and liquid phases [16].

The difference in phase behaviour of the two systems investigated may underlie a regulatory mechanism available to the cell in triggering or directing membrane-related processes. The lipid environment is of paramount importance for the function of the transmembrane proteins, and one can speculate on several possible mechanisms that would ensure that the appropriate lipid composition is selected. For instance, one of the possible scenarios discussed widely in the literature is the effect of the transmembrane proteins in selecting and organizing their immediate lipid environment through generic and specific interactions [2]. If, however, the membrane composition is indeed close to a liquid–liquid (L_o–L_α) miscibility critical point as has already been suggested [10, 15–17], crossing that boundary offers an alternative mechanism for creating a heterogeneous lateral organization in the plane of the membrane, the different phases of which could accommodate or activate the desired protein action. But this change in the membrane mesostructure will bring about a related change in the membrane mechanical properties, as suggested by our model experiments, which could have its own effect of promoting or suppressing protein stability, conformation and function. If this mechanism is feasible at all, it seems to offer a convenient way for the cell to regulate membrane composition, structure and function on appropriate timescales and length scales. In this respect, it is important to note that plasma membrane lipid rafts are much smaller than lateral domains in artificial vesicles (sub-200 nm in the former versus μm in the latter) and are believed to have much shorter lifetime (seconds at most versus minutes) [2]. It would therefore be important to study the elastic properties of membranes containing submicrometre rafts and how the longer timescale membrane dynamics are affected by rapid raft formation and disassembly.

5. Conclusions

We studied the effect of an in-plane liquid–liquid phase separation on the bending modulus of vesicles composed of ternary mixtures of DOPC, DPPC and cholesterol. Above the phase transition temperature (T_c), the ternary lipid membranes are in a uniform liquid state and show large thermal fluctuations. Using the contour detection technique in video microscopy, we measured the bending moduli for these systems. The main result is that laterally separated membranes (at $T < T_c$) of composition 1:1 DOPC:DPPC + 30 mol% cholesterol are significantly stiffer than homogeneous membranes of 1:1 DOPC:DPPC + 60 mol% cholesterol. At higher temperatures ($T > T_c$), where both compositions are in a uniform phase, the bending moduli are the same. These experiments show that the effective membrane bending modulus is sensitive to the onset of the phase separation in the membrane. It remains to be seen whether this conclusion will also hold true for nanometre-sized lipid domains, below the optical resolution limit. We have measured the mechanical properties of coexisting phases directly near the critical point ($T \approx T_c$), finding that the volume constraint is important in determining the vesicle morphology. We speculate that the coupling between the membrane composition and the membrane bending rigidity may play a role in

controlling the biological function of embedded proteins, due to the proximity of the membrane lipid composition to a thermodynamic critical point.

Acknowledgments

References

[1] Dowhan W 1997 *Annu. Rev. Biochem.* **66** 199–232
[2] Devaux P and Morris R 2004 *Traffic* **5** 241–6
[3] Helfrich W 1973 *Z. Naturf. Biosci.* C **28** 693–703
[4] Alberts B, Bray D, Lewis J, Raff M, Roberts K and Watson J D 1994 *Molecular Biology of the Cell* (New York: Garland Publishing)
[5] Boal D 2002 *Mechanics of the Cell* (Cambridge: Cambridge University Press)
[6] Dobereiner H, Dubin-Thaler B J, Giannone G, Haluska C K, Petrov P G, Reinecke A, Riske K and Sheetz M P 2005 *Adv. Solid State Phys.* **45** 71–82
[7] Engelman D 2005 *Nature* **438** 578–80
[8] Discher D and Eisenberg A 2002 *Science* **297** 967–73
[9] Findlay H and Booth P 2006 *J. Phys.: Condens. Matter* **18** S1281–91
[10] London E 2005 *Biophys. Acta* **1746** 203–20
[11] Tillman T and Cascio M 2003 *Cell Biochem. Biophys.* **38** 161–90
[12] Turner M and Sens P 2004 *Phys. Rev. Lett.* **93** 118103
[13] Laan E, Killian J and Kruijff B 2004 *Biochim. Biophys. Acta* **1666** 275–88
[14] Lundbaek J 2005 *Mol. Pharmacol.* **68** 680–9
[15] Veatch S L and Keller S L 2002 *Phys. Rev. Lett.* **89** 268101
[16] Veatch S L and Keller S L 2005 *Biochim. Biophys. Acta* **1746** 172–85
[17] McConnell H M and Vrljic M 2003 *Annu. Rev. Biophys. Biomol. Struct.* **32** 469
[18] Cicuta P, Keller S L and Veatch S L 2007 *J. Phys. Chem.* B **111** 3328
[19] Lecuyer S and Charitat T 2006 *Europhys. Lett.* **75** 652
[20] McMullen T, Lewis R and McElhaney R 2004 *Curr. Opin. Colloid Interface Sci.* **8** 459–68
[21] Ohvo-Rekila H, Ramstedt B, Leppimaki P and Slotte J P 2002 *Prog. Lipid Res.* **41** 66–97
[22] Honerkamp-Smith A R, Cicuta P, Collins M D, Veatch S L, den Nijs M, Schick M and Keller S L 2008 *Biophys. J.* **95** 236–46
[23] Semrau S, Idema T, Holtzer L, Schmidt T and Storm C 2008 *Phys. Rev. Lett.* **100** 088101
[24] Veatch S L, Cicuta P, Sengupta P, Honerkamp-Smith A R, Holowka D and Baird B 2008 *ACS Chem. Biol.* **3** 287
[25] Angelova M I, Soleau S, Meleard P, Faucon J F and Bothorel P 1992 *Prog. Colloid Polym. Sci.* **89** 127–31
[26] Pecreaux J, Dobereiner H G, Prost J, Joanny J F and Bassereau P 2004 *Eur. Phys. J.* E **13** 277–90
[27] Helfrich W and Servuss R M 1984 *Nuovo Cimento* D **3** 137–51
[28] Yoon Y-Z, Hong H, Brown A, Kim D C, Kang D J, Lew V L and Cicuta P 2009 *Biophys. J.* **97** 1606–15
[29] Henriksen J, Rowat A C and Ipsen J H 2004 *Eur. Biophys. J.* **33** 732–41
[30] Julicher F and Lipowsky R 1996 *Phys. Rev.* E **53** 2670–83
[31] Lipowsky R 1992 *J. Physique* II **2** 1825–40
[32] Yanagisawa M, Imai M, Masui T, Komura S and Ohta T 2007 *Biophys. J.* **92** 115–25
[33] Semrau S, Idema T, Schmidt T and Storm C 2009 *Biophys. J.* **96** 4906–15
[34] Evans E and Rawicz W 1990 *Phys. Rev. Lett.* **64** 2094–7
[35] Baumgart T, Das S, Webb W W and Jenkins J T 2005 *Biophys. J.* **89** 1067–80
[36] Veatch S L, Polozov I V, Gawrisch K and Keller S L 2004 *Biophys. J.* **86** 2910–22
[37] Niggemann G, Kummrow M and Helfrich W 1995 *J. Physique* II **5** 413–25
[38] Lee C H, Lin W C and Wang J P 2001 *Opt. Eng.* **40** 2077–83
[39] Pan J, Mills T T, Tristram-Nagle S and Nagle J F 2008 *Phys. Rev. Lett.* **100** 198103